

# Wind vibration energy harvesting through macro fiber composites: a probabilistic approach

Abhishek Ghiya<sup>a,\*</sup>, A. Arockirajan<sup>b</sup>, Sayan Gupta<sup>b</sup>

<sup>a</sup>Research and Development Establishment, DRDO, Pune, India

<sup>b</sup>Department of Applied Mechanics, IIT Madras, Chennai, India

\*Corresponding author: abhi.nitjai@gmail.com

## Keywords

MFC  
PZT  
Finite element  
Wind vibration  
Probabilistic approach

Received: 03-11-2014

Revised: 26-11-2015

Accepted: 06-01-2016

## Abstract

Piezoelectric materials such as Macro Fiber Composites (MFC) have certain advantages such as flexibility and high endurance strength over bulk piezoelectric materials. An experiment and simulation based study is presented here for a P2 type (d31 effect) MFC patch for wind energy harvesting. A single cantilever beam configuration has been tested under harmonic and random (wind vibrations) excitations. Wind vibration test was done inside a wind tunnel for Beaufort scale level 5, which is the most common environmental condition. An average power density of  $33.2 \mu\text{W}/\text{cm}^3$  and  $1.32 \mu\text{W}/\text{cm}^3$  has been obtained from harmonic and wind vibration, respectively. A reliable and accurate Finite Element (FE) model has been created for simulating the output voltage. Probabilistic approach has been used to analyse and predict the output voltage data from the wind vibration experiment.

## 1 Introduction

Unused power exists in various forms such as solar energy, thermal gradients, acoustic and mechanical vibrations. The field of power harvesting has experienced significant growth over the past few years due to the ever-increasing desire to produce self-powered portable and wireless electronics. Vibration-based energy harvesting has received growing attention over the last decade. The main advantages of piezoelectric materials in energy harvesting compared to two other transduction mechanisms i.e. electrostatic and electromagnetic, are their high power densities and ease of application. In piezoelectric material, the output voltage results from the constitutive behaviour of the material, which eliminates the requirement of an external power source. These advantages make piezoelectric materials the preferred choice for energy harvesting. Minh *et al.* [2011] used a piezo-composite generating element (PCGE) to

generate the electric power [Minh *et al.* 2011]. The purpose of the study was to introduce a small-scale windmill that can work in urban areas. The device produced 8 mW Peak power and was able to charge a 40 mAh battery.

In this work, the concept of harvesting wind energy through MFC has been explored. A cantilever beam configuration has been tested for harmonic and random (wind) vibrations. The focus has been on quantifying and maximizing the electrical energy generated from the flexure of a single piezoelectric device bonded over a cantilever beam and subjected to wind induced vibrations. Although the monolithic PZT has higher piezoelectric coupling coefficient than the MFC patch, due to flexibility and higher endurance in cyclic loading [Yaowen *et al.* 2009; Henslee *et al.* 2012; Wilkie *et al.* 2000; Zhang *et al.* 2006], MFC patch has been selected for harvesting energy from wind vibrations. Two preferred modes for energy harvesting from MFC are d33 and d31. Although

the value of  $d_{33}$  is more than  $d_{31}$  but the P2 type MFC is especially suited for energy harvesting applications due its higher capacitance and more charge generation at the same strain level compared with the P1 device [Roundy *et al.* 2003].

First, laboratory scale experiments were carried out to examine the performance of MFC in generating energy from deterministic loads such as low frequency harmonic vibrations. A P2 type (in  $d_{31}$  mode) MFC patch has been tested under harmonic vibration. These test results were also used to validate the FE model. To explore the energy harvesting capability under more realistic environment, i.e. actual wind vibrations (random vibrations), the same harvester has been experimentally tested inside an open circuit wind tunnel at different wind speeds. Five different environmental conditions have been simulated inside the wind tunnel based on Beaufort scale. Velocity and output voltage data have been logged through data acquisition system. As the output voltage from experiments was in the form of a random signal, probabilistic approach has been used to analyze the signal and predict the output voltage with some certainty.

A reliable and accurate FE model has been developed to simulate the output voltage from MFC patch. For FE modelling and analysis, commercial software, ANSYS, has been used. MFC has been modelled as a layered material. Equivalent properties have been calculated for the active layer, which is a composites lamina of PZT-5A1 fiber and epoxy. Drag force on the beam has been calculated using velocity data from experiments. Output voltage, from FE simulations has been compared with experimental values. A good match was found between experimental results and simulation results, thus the validated FE model can be used to predict energy output and parametric study for different load cases.

## 2 Experimental setup

A schematic diagram of a single harvester is shown in Figure 1. A MFC P2 type patch has been bonded at the end of the beam. A two component adhesive (recommended by Smart-material Corp.) 3M-DP-460 was used to paste MFC patch over aluminum beam. The type of adhesive and proper adhesion plays very important role in transfer of strain from beam to the patch. Vacuum bagging process has been used to

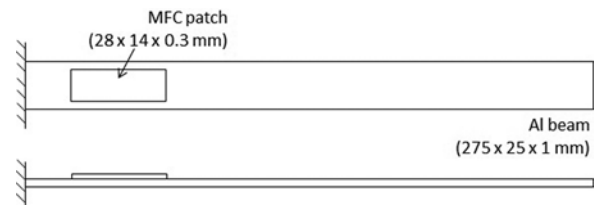


**Figure 1.** Schematic diagram of the cantilever beam harvester.

achieve good bonding between the MFC patch and the aluminum beam.

Figure 2 shows the schematic of experimental setup for the harmonic excitation. A sinusoidal excitation was given by an Agilent make signal generator to a Data Physics make shaker (model no. GW-V4/PA30E). The same was transmitted to the beam via stinger. A Dytran make force sensor (model no. 1053V1) was attached on top of the stinger, which measures force transmitted to the beam by the shaker. Response of the beam is measured through a Dytran make miniature accelerometer (model no. 3225F), which is attached to the free end of beam. A 4-channel Dytran make current source (model no. 4114B1) is used as a signal conditioner for the force sensor, impact hammer and accelerometer. Data logging from force sensor, accelerometer and MFC patch has been done through a HBM make data acquisition system (model no. DQ401). Figure 3 shows the instrumentation involved in the experiment. A professional grade multimeter is also used to measure open circuit rms voltage from MFC patch.

Wind vibration experiments have been conducted inside an open circuit wind tunnel. Figure 4 shows the schematic diagram for the wind vibration test setup. Inside view of test section is shown in Figure 5. The setup consists of a cantilever beam bonded with MFC patch (Figure 1), mounting fixture, velocity sensor, DAQ and wind tunnel. The cantilever harvester has been placed perpendicular to wind flow direction. Air was sucked from contraction cone towards test section by a fan driven

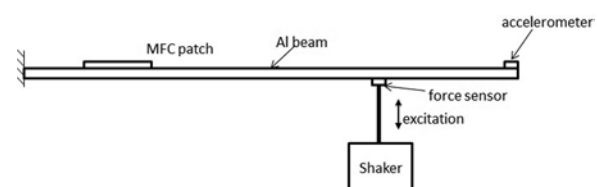


**Figure 2.** Schematic diagram of the harmonic excitation experiment.

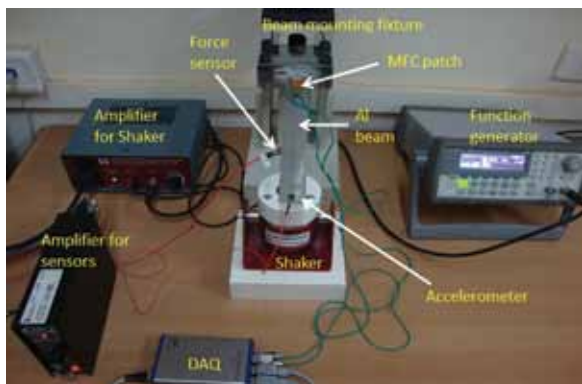


Figure 3. Experimental setup for harmonic excitation.

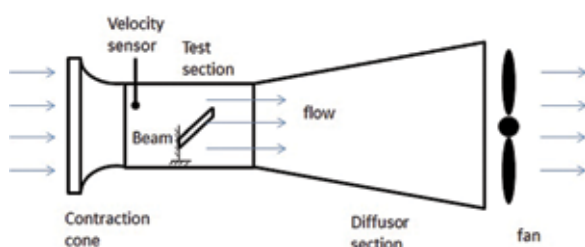


Figure 4. Schematic diagram of the open circuit wind tunnel.

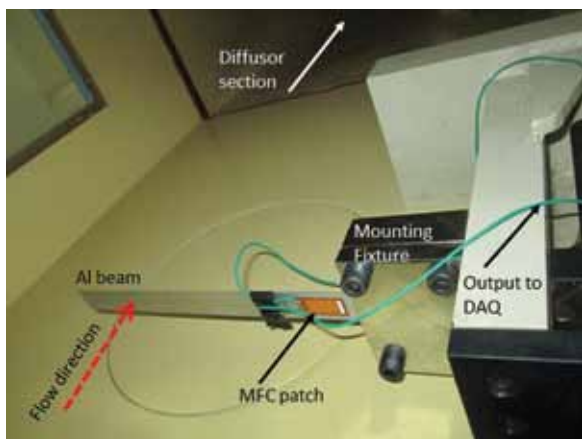


Figure 5. Test section of wind tunnel.

by an AC motor. Air speed was controlled by an electronic controller and measured by the velocity sensor. Experiments have been carried out at five different air speeds to investigate energy output at different environment condition.

### 3 Finite element modeling

A detailed Finite element model has been created to simulate the energy harvesting from MFC

patch in  $d_{31}$  mode. Commercial software ANSYS has been used for FE modelling and simulation. Viscous damping was modelled using Rayleigh parameters obtained from experiments. Coupled dynamic analysis was done with full integration method to simulate energy output. To increase the accuracy and reduce the approximation, a layered FE model has been created. Figure 6 shows the side view of beam with MFC patch. A zoomed in view show details of different layers modelled over the thickness. The MFC patch is modelled as a material having five layers. Solid 5 element having piezoelectric modelling capability has been used to model active layer (PZT 5A1 fiber + epoxy). It is an 8-node, brick type element and has four degree of freedoms per node, three translation  $u_x$ ,  $u_y$ , &  $u_z$  and one voltage degree of freedom.

Layered solid 185 element having three translational degree of freedoms per node was used to model adhesive, kapton & epoxy, below active layer. It is a brick type, 8-node element. Same element was used to model epoxy & kapton, above active layer. Solid 185 element (in monolithic form) is used to model aluminum beam. Figure 7 shows the mesh of MFC patch. FE model of the harvester has 149766 numbers of elements. Active layer has PZT-5A1 fiber (Sonox-P502) as reinforcement and epoxy as matrix.

As it is very difficult to model each fiber and epoxy surrounding it, active layer is modeled as a single orthotropic material. The equivalent properties of the orthotropic lamina were calculated by mechanics of materials approach in micro-mechanics. This approach is based on the representative volume element (RVE), which is the smallest region or piece of material over which the stresses and strains can be regarded as macroscopically uniform and yet maintains fiber to

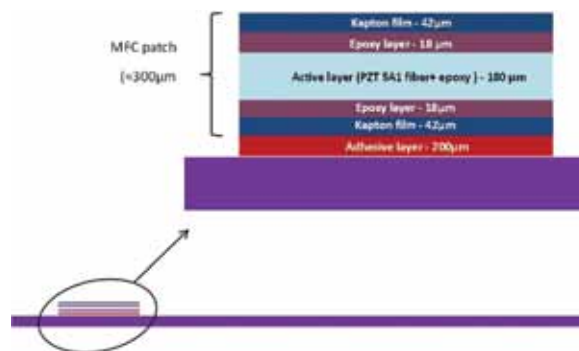
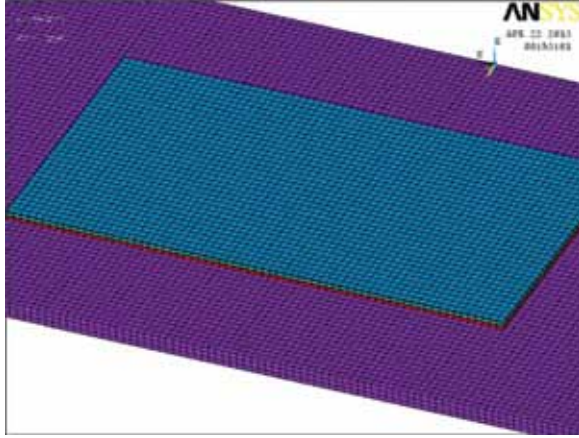


Figure 6. Details of layers modeled in FE model.



**Figure 7.** Mesh near MFC patch.

matrix volume ratio identical to parent composite material. These conditions allow considering the RVE as a point of the macrostructure and thus determining homogenised properties that are valid for every point of the material. The concept of RVEs was introduced by Hill in [1963]. Berger *et al.* [2003; 2005] has compared the RVE method with analytical Asymptotic Homogenization Method (AHM) for calculation of effective coefficients for piezoelectric fiber composites and found good coincidence between both methods. Medeiros *et al.* [2012] has calculated the effective properties for smart composite materials with piezoelectric fibers made of PZT embedded in epoxy resin through RVE approach and found that the results are comparable with other methods reported in the literature and also to results previously published.

Using fiber volume fraction  $v_f = 0.85$  [smart.material.com], properties of PZT-5A1, properties of epoxy and formulae for equivalent properties, equivalent properties were calculated for active layer. Table 1 shows the equivalent properties for the active layer. Formulae for calculating equivalent coupling coefficients are taken from Deraemaeker *et al.* [2009]. Table 2 shows the mechanical properties for other materials.

All translational displacement degree of freedom ( $u_x$ ,  $u_y$  and  $u_z$ ) of beam end, nearer to MFC patch were fixed. Electrodes were defined on top and bottom surface of the active layer. Electrode on top surface was defined by coupling voltage degree of freedom of all nodes on the top surface. Similarly the bottom electrode was defined by coupling voltage degree of freedom of all nodes on bottom surface. To ground

**Table 1.** Material properties for active layer.

**PZT-5A1 (85%) + Property epoxy (15%)**

Mechanical properties	$E_{11}^E = 47.17$ Gpa, $E_{22}^E = 16.98$ GPa $E_{33}^E = 42.229$ Gpa, $G_{12}^E = 6.032$ GPa $G_{31}^E = 17$ Gpa, $G_{32}^E = 6.06$ GPa $\nu_{12} = 0.395$ , $\rho = 6917$ kg/m <sup>3</sup>
Coupling coefficients	$d_{31} = -181 \times 10^{-12}$ C/N $d_{32} = -153 \times 10^{-12}$ C/N $d_{33} = 435.25 \times 10^{-12}$ C/N $d_{15} = d_{24} = 560 \times 10^{-12}$ C/N* (*kept same)
Relative dielectric properties	$\epsilon_{33}^r = 1573.13$

**Table 2.** Material properties for other materials.

Material	Young's modulus (GPa)	Poisson's ratio	Density (kg/m <sup>3</sup> )
Aluminum	70	0.3	2750
Epoxy	2.5	0.3	1100
Kapton	2.8	0.3	1580
Adhesive	0.5	0.3	3000

the bottom electrode a zero potential was applied on all the nodes.

## 4 Results & discussion

### 4.1 Modal analysis

Modal parameters such as natural frequencies and Rayleigh damping factors were determined from experimental modal analysis through impact hammer test. Figure 8 shows the Fast Fourier Transform (FFT) of the measured response during the impact test. First three damped natural frequencies can be determined from the peaks observed in the figure. Some secondary effects can be seen in the FFT figure near to 1st resonance frequency. This may be due to components like printed circuit board (PCB) patch near MFC patch, lead wires or even due to MFC patch.

An estimate of the undamped natural frequencies can be obtained from the relation  $\omega_n = \omega_d / \sqrt{1 - \xi^2}$ , where,  $\xi$  is the damping ratio.

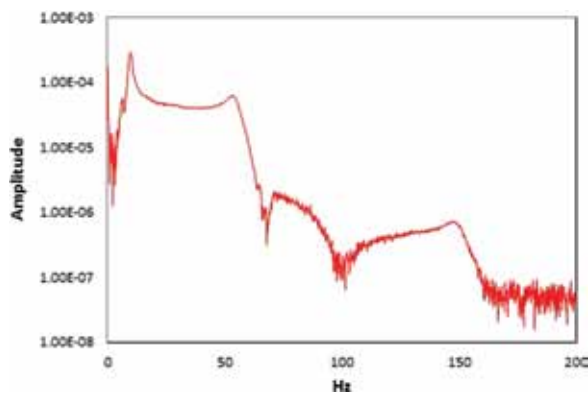


**Figure 8.** FFT of the response due to impulse excitation.

An estimate of  $\xi$  is obtained from the free vibration response of the beam and calculating the logarithmic decrement ratio. This is calculated by noting the amplitudes of any two peaks,  $n$  cycles apart, and using the relation for logarithmic decrement ( $\delta$ )

$$\delta = \frac{1}{n} \ln \left( \frac{a_0}{a_n} \right) = \frac{2\pi\xi}{\sqrt{1-\xi^2}} \quad (1)$$

where,  $a_0$  and  $a_n$  are the amplitude of the peaks,  $n$  cycles apart. The value of  $\xi$  is found to be 0.1 from Eq. 1. Table 3 shows the comparison of first three undamped natural frequencies (at open circuit) determined from analytical calculations, experiments and FE simulations.

The damping matrix for Rayleigh damping model (proportional damping) can be written as

$$\mathbf{C} = \alpha\mathbf{M} + \beta\mathbf{K} \quad (2)$$

where  $\alpha$  and  $\beta$  are mass ( $\mathbf{M}$ ) and stiffness ( $\mathbf{K}$ ) are proportionality damping constants respectively. These constants can be calculated from

$$\xi_i = \frac{\alpha}{2\omega_i} + \frac{\beta\omega_i}{2} \quad (3)$$

**Table 3.** Comparison of undamped natural frequencies.

Natural frequency	Analytical	Experiment	FE
$f_1$ (Hz)	9.72	9.69	10.116
$f_2$ (Hz)	60.72	53.35	61.261
$f_3$ (Hz)	170.2	147.08	168.06

For  $i = 1$  and 2 and assuming  $\xi_1 = \xi_2$ , two linear algebraic equation can be obtained between  $\alpha$  and  $\beta$ . Value of  $\alpha$  and  $\beta$  is found to be 10.219 and  $5.249 \times 10^{-4}$  respectively. These parameters were used in dynamic FE simulations of energy harvesting.

## 4.2 Harmonic vibrations

To determine the energy output from MFC patch at low frequencies a sinusoidal force of 12 Hz frequency, which is nearer to the first natural frequency, was applied through a shaker. The reason for choosing 12 Hz frequency instead of 1st resonance frequency ( $\approx 10$  KHz) is to avoid resonance which in turn would induce geometrically nonlinear effects in the beam. Figure 9 shows the applied force profile. Same force profile has been used for simulating energy harvesting under a harmonic force in FE. Figure 10 compares experimental and simulated open circuit voltage output from MFC patch under harmonic load. Qualitatively both are in good agreement but the peak output voltage obtained from experiment is around 15% lower than the simulated peak output voltage. Therefore the FE model can be assumed to be realistic and fairly accurate. The model can be used for parametric studies and simulating output voltage for complex loads such as wind vibrations. The difference between experimental and simulated output voltage (Figure 10) can be due to the fact that in FE simulation a perfect bond was modelled between the beam and the MFC patch, which ensures a perfect strain transfer. But in the specimen under consideration, this may not be the case. Another reason is the inaccuracies related to modelling of the damping.

To find the maximum output power and internal impedance of MFC patch, experiments

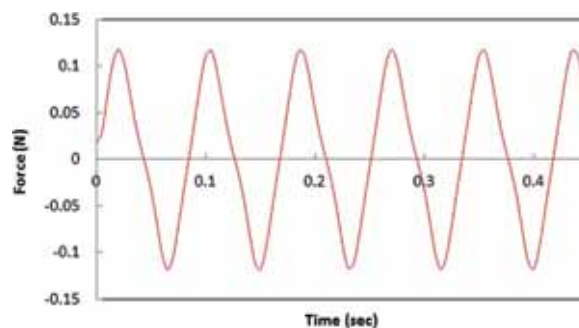


**Figure 9.** Applied force profile.

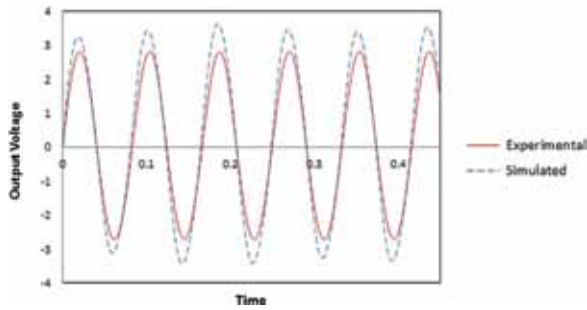


**Figure 10.** Comparison of open circuit output voltage.

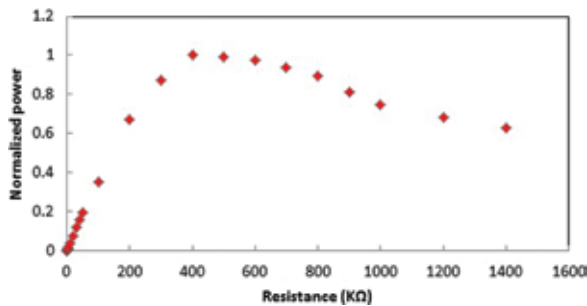


**Figure 11.** Variation in output power with external resistive load.

have been carried out at harmonic excitation shown in Figure 9. A variable resistor was used as an external electrical load. Figure 11 shows the variation of power harvested from MFC patch at various resistance values. Output power has been normalized with respect to maximum value.

At 400 kΩ output power was maximum, so internal impedance of MFC patch is  $\approx 400$  kΩ.  $I_{rms}$  is 3.13  $\mu A$  and average power calculated by above equation is 3.91  $\mu W$  at 400 KΩ resistance. Peak output power ( $P_{peak} = P_{avg} \times 2$ ) 7.82  $\mu W$  and average power density 33.2  $\mu W/cm^3$  was obtained.

### 4.3 Wind vibration

Experiments have been carried out at level 5 (fresh breeze condition) of Beaufort scale which is the most common environment condition. Table 4 lists velocity at which experiment was carried out and corresponding peak and rms output voltage. The applied excitation (velocity) and output voltage is a random signal; analysis of input signal and output signal has been done in frequency domain. Power spectral density (PSD) was calculated and analyzed for input excitation and output voltage. Figure 12 shows PSD plot of velocity data, which shows that the excitation

**Table 4.** Experimental results for wind vibration.

Air mean speed (m/s)	Peak voltage (volts)	RMS of voltage (volts)	Beaufort scale
8.4973	1.511	0.415	5 – Fresh breeze

signal is pretty much a broadband signal containing all frequencies (random vibration). Figure 13 shows PSD plot of output voltage, which shows that five natural modes are excited by air flow but 1st mode produces peak output.

Also, for predicting certain output voltage from MFC, probabilistic approach has been used. Probability density function (PDF) was plotted and studied for this case. PDF describes the relative likelihood for a random variable (output voltage) to take on a given value. The probability of the output voltage falling within a particular range of values is given by the integral of PDF over that range, that is the area under PDF curve within the desired range. The total area under the PDF curve is always one. Also, the root mean square (RMS) value can be calculated from PDF. The RMS value is shown in Table 4. Figure 14

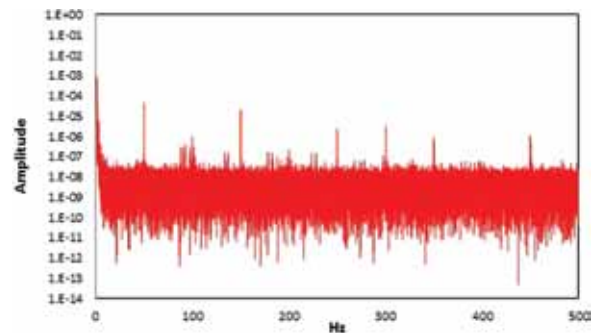


**Figure 12.** PSD plot for Velocity.

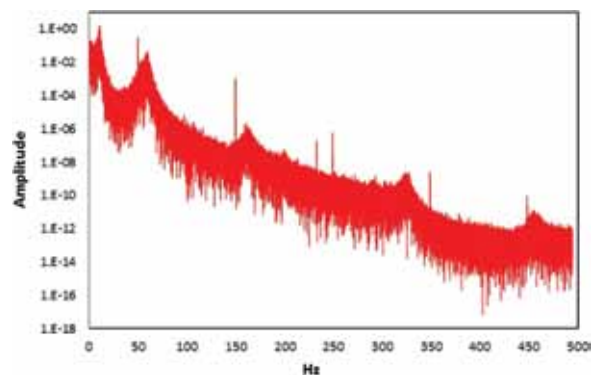


**Figure 13.** PSD plot for output voltage.

shows PDF of output voltage. From the plot, the probability of achieving a range of output voltage can be found out. The probability of achieving output between 0.2 to 0.42 volt is 0.5 for this case. This probability data is very useful in designing the storage device (capacitor or battery) and its charging time.

Power output was also calculated at 400 k $\Omega$  resistance. Peak and average power are 2.054  $\mu$ W and 0.1552  $\mu$ W respectively, which is very small as compare to harmonic load case. The power density for this case is 1.32  $\mu$ W/cm<sup>3</sup>. So in more realistic conditions (random vibrations) energy output is very small as compare to ideal lab conditions. The power output is not enough to power a typical MEMS sensor. An array of such harvesters can provide sufficient output to power a sensor. FE simulation was also carried out, using the drag force calculated from the experiment.

Formula for drag force is

$$F_D = \frac{1}{2} \rho A C_D (v(t))^2 \quad (4)$$

where,  $F_D$  is the drag force in the direction of flow velocity,  $\rho$  is the mass density of air,  $v(t)$  is the velocity of the object relative to the air, which is air velocity in this case,  $A$  is the exposed area and  $C_D$  is the coefficient of drag. *Drag coefficient* is a dimensionless coefficient related to the object's geometry and taking into account both skin friction and form drag. For the experiments, following data has been used. Mass density for air is 1.1 kg/m<sup>3</sup> (kg/m<sup>3</sup>),  $v(t)$  = velocity time history obtained from velocity sensor, beam surface area is 275  $\times$  25 mm<sup>2</sup>. Coefficient of drag is taken as 1.98 by assuming the beam as a 2D plate. As the thickness of the beam is very small as compare to length, this assumption is reasonable one.

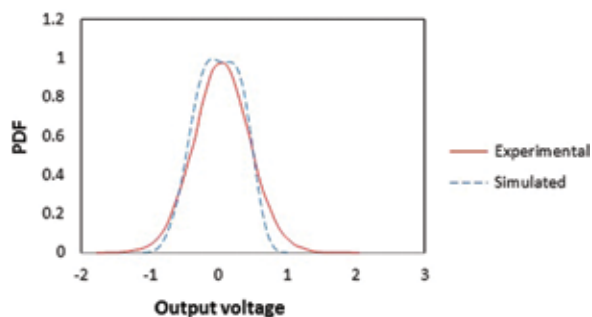


Figure 14. Comparison of PDF for output voltage.

Figure 14 gives the comparison of PDF between experimental and simulated results. The simulated and experimental result matches quite well. So the FE model was validated for complex loads as well. The model can be used for parametric study and for estimating an accurate output voltage for different load cases.

## 5 Conclusions

A P2 type MFC patch is investigated for energy harvesting under harmonic and wind load. Probabilistic approach was used to analyze the data from wind vibration experiments. For the most common environment condition related to wind, the peak and RMS output voltage are 1.511 and 0.4153 volts respectively. Peak and average output power are 2.054  $\mu$ W and 0.1552  $\mu$ W respectively. A moderate power density 1.32  $\mu$ W/cm<sup>3</sup> was obtained. An accurate FE model was developed and the results match quite well in both types of loads – harmonic and random. To increase the power output from wind vibrations, shape and size of the beam can be optimized to achieve maximum drag force. An array of MFC harvesters in series may be explored to increase the output power. The work and concepts presented in this paper is an ongoing work being carried out in Applied Mechanics department of IIT Madras.

## Acknowledgements

I would like to thank Dr. Shaikh Faruque Ali and Dr. Pijush Ghosh for their support in the experiments. I also want to express my gratitude towards Dr. Sunetra Sarkar, Sandip and Venkatramani for their support in wind tunnel test, carried out in Department of Aerospace Engineering, IIT Madras.

## References

- ANSYS 13.0 User Manual.
- Berger, H, *et al.* (2003) Finite element and asymptotic homogenization methods applied to smart composite materials. *Comput Mech.* **33**, 61–7.
- Berger, H, *et al.* (2005) Calculation of effective coefficients for piezoelectric fiber composites based on a general numerical homogenization technique. *Composite Structures.* **71**, 397–400.

- Deraemaeker, A., Nasser, H., Benjeddou, A. and Preumont, A. (2009) Mixing Rules for the Piezoelectric Properties of Macro Fiber Composites. *Journal of Intelligent Material Systems and Structures*. **20**, (12) 1475–1482.
- Henslee, I., Miller, D.A. and Tempero, T. (2012) Fatigue life characterization for piezoelectric macro-fiber composites. *Smart Materials and Structures*. **21**, (10) 105037.
- Hill, R. (1963) Elastic properties of reinforced solids: some theoretical principles. *Journal of the Mechanics and Physics of Solids*. **11**, 357–372.
- Medeiros, *et al.* (2012) Effective Properties Evaluation for Smart Composite Materials. *J of the Braz Soc of Mech Sci & Eng*. **XXXIV**.
- Minh, C., Tien, T. and Goo, N.S. (2011) Use of a piezo-composite generating element for harvesting wind energy in an urban region Use of a piezo-composite generating element for harvesting wind energy in an urban region. *Aircraft Engineering*.
- Roundy, S., Wright, P.K. and Rabaey, J. (2003) A study of low level vibrations as a power source for wireless sensor nodes. *Comput Commun*. **26**, 1131–44.
- Smart-material.com, morgan-electroceramics.com
- Wilkie, W., High, J. and Bockman, J. (2000) Reliability Testing of NASA Piezocomposite Actuators.
- Yaowen Yang, Lihua Tang, and Hongyun Li. (2009) Vibration energy harvesting using macro-fiber composites. *Smart Mater Struct*. **18**, 115025.
- Zhang, X.P., Ye L., Mai Y. and Galea S. (2006) Fatigue Crack Growth and Piezoelectric Property Decay Induced By Cyclic Electric Fields For An Actuation Piezoceramic. *SIF2004 Structural Integrity and Fracture*.



**Abhishek Ghiya** received his B.Tech. degree in Mechanical Engineering from MNIT, Jaipur in 2005. He obtained his M.Tech. degree in Applied Mechanics from IIT Madras in 2013. He is currently working as Scientist in Composites Research Centre, Research and Development Establishment (Engrs.), DRDO, Pune. His areas of work are FRP composites, piezoelectric materials and MEMS devices.



**Prof Sayan Gupta** is a faculty member in the Department of Applied Mechanics, Indian Institute of Technology Madras. His research interests are in the areas of vibrations, stochastic mechanics and nonlinear dynamics. More information about the research undertaken by him and his group – The Uncertainty Lab – is available at <https://apm.iitm.ac.in/smlab>.



**A. Arockiarajan** is an Associate Professor in the Department of Applied Mechanics at the Indian Institute of Technology Madras, India. He received his Ph.D. in 2005 from University of Kaiserslautern, Germany. His current fields of interests are intelligent and smart structures, nonlinear piezoelectric and ferroelectric materials, composite and sandwich structures.